

## Whole-rock geochemical compositions of Miocene sedimentary and volcanic rocks from the Izumo–Matsue districts and Shimane Peninsula, SW Japan

Barry Roser\*, Yoko Tateishi\* and Katsuhiko Nakayama\*

### Abstract

Miocene backarc clastic sediments crop out in a strip along coastal Shimane prefecture between Izumo and Matsue, and in Shimane Peninsula. New XRF analyses of 147 sandstones, mudrocks and associated volcanic rocks from the Koura, Ushikiri, Omori, Fujina, Jinzai and Matsue Formations show considerable compositional variation occurs over relatively short stratigraphic intervals. Koura Formation sandstones have Upper Continental Crust (UCC) –normalized multielement patterns intermediate between interbedded felsic tuff and coeval andesite. Turbidite sediments from the Ushikiri Formation at Chikumi also have andesitic patterns, but shallow water equivalents in the Omori Formation near Izumo exhibit dacitic signatures identical to the volcanic rocks on which they rest. Elemental abundances in the overlying Fujina Formation are depleted relative to UCC, suggesting influx of weathered plutonic detritus. Similar signatures occur in the Jinzai Formation, except for localized basaltic contributions around the Jinzai Basalt edifice. Sediments of the Matsue Formation, which is correlative with the Jinzai Formation, also have depleted patterns indicative of plutonic source, but carry signatures suggestive of more intense source weathering and more advanced sorting in a shallower water depositional environment. The stratigraphic and lateral variations observed reflect relatively proximal deposition, complex source geology, and sediment supply from restricted catchments.

### Introduction

Neogene sedimentary, volcanic and lesser intrusive rocks crop out extensively in the Izumo–Matsue district and in Shimane Peninsula, forming a coastal strip adjoining a largely Paleogene intrusive basement that forms uplands to the south (Fig. 1). The sediments were deposited in a rifted backarc basin during and after the Early to Early middle Miocene opening of the Japan Sea (Kano, 1998). The Miocene sequence in the area has been the subject of numerous studies which have spanned many aspects of its general geology, sedimentology, and paleontology (e.g. Takayasu, 1986; Kano *et al.*, 1989; 1991; 1994; 1997; Morita and Nakayama, 1999). The succession is thus well mapped, and a broad stratigraphy has been established.

Geochemical studies of clastic sediments have become common in recent years, as an additional lever to help understand the provenance, tectonic setting and evolution of sedimentary sequences. The environments examined in such work range from immature volcanic arcs through to passive continental margins. Very few studies, however, have specifically examined the composition of sediments deposited in known or demonstrable backarc settings. Geochemical signatures of sedimentary successions deposited in this environment are thus not well known.

The Miocene succession in west Shimane Prefecture gives a good opportunity to examine the compositions of backarc sediments, because its backarc setting is clearly established. Although several geochemical studies of

sediments have been carried out in this area, they have focussed on the compositions of shales, and data for sandstones are lacking. As a first step in fully characterizing the geochemical signatures of the Miocene succession in this area, we have acquired comprehensive whole-rock XRF data for a collection of 147 sandstones and mudrocks from the Izumo district, Matsue City, and Shimane Peninsula (Fig. 1). Most of the samples are from the Omori, Fujina, Jinzai and Matsue Formations (Izumo and Matsue), with a lesser number from the Ushikiri and Koura Formations in Shimane Peninsula. A small number of analyses of coeval volcanic rocks are also included in the database, to permit evaluation of potential source compositions.

The primary purpose of this report is to outline the coverage of the sample suite and to present the raw data, for later use in a more detailed interpretive paper. However, we also briefly examine the geochemical variability within the database. The results show substantial geochemical variation within relatively narrow stratigraphic intervals, reflecting the proximal nature of the sediments and the geologic complexity of their source.

### Stratigraphy and Geology

Schematic stratigraphy of the Miocene succession in the areas examined is given in Figure 2. The basal unit in Shimane Peninsula, the early Miocene Koura Formation, consists primarily of non-marine sandstone, conglomerate and laminated mudstone. Some andesitic to rhyolitic tuffs and breccias also occur. The Koura Formation is conformably overlain by the early-middle Miocene Josoji

\*Department of Geoscience, Shimane University, Matsue 690–8504

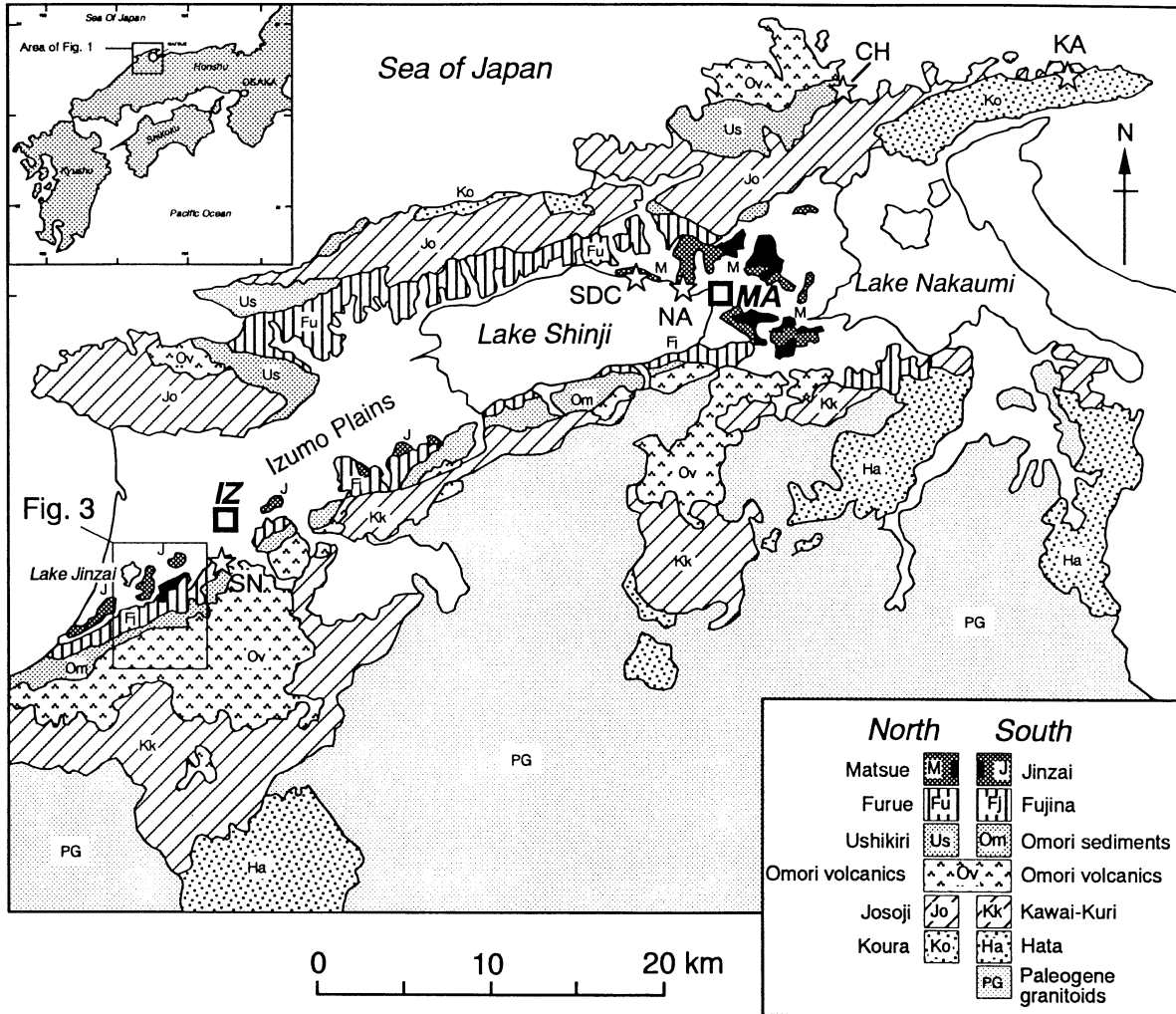


**Fig. 1.** Map showing the location of the areas sampled, and generalized distribution of Miocene sedimentary and volcanic rock units. Geology based on the 1:200,000 geological map of Shimane Prefecture (Editorial Board of Geological map of Shimane Prefecture, 1997). Inset: location in Japan. Box: area of Figure 3. Locality abbreviations: IZ–Izumo City; MA–Matsue City. Stars (sample sites) SDC–Shimada drillcore; NA–Nanpeidai, CH–Chikumi; KA–Karuba; SN–South Nishi–Izumo.

Formation, which comprises black argillaceous marine sediments and intercalated submarine rhyolitic to andesitic lavas, hyaloclastites and pyroclastic deposits (Kano and Nakano, 1986). In that area it is succeeded by the middle Miocene Ushikiri Formation, which consists dominantly of volcanoclastic and tuffaceous sandstone, interbedded mudstone and lesser conglomerate. Deposition of the coarser sediments was from turbidity currents or debris flows (Kano *et al.*, 1989). Paleocurrent indicators in west Shimane Peninsula show derivation from the southeast (Kano *et al.*, 1991), and the Ushikiri Formation there is thus likely to be the deeper-water equivalent of the more proximal Omori Formation in the Iwami-Oda-Izumo area. However, paleocurrents in east Shimane Peninsula (Chikumi) are much more varied, with various sets indicating derivation from the west, and from the north to northeast (Yamauchi *et al.*, 1980; Yamauchi and Yoshitani, 1981). This suggests that this part of the Ushikiri Formation

had a different source from that in the west of the peninsula. The Ushikiri Formation in Shimane Peninsula is succeeded by the Furue Formation, which consists of massive argillaceous rocks, also of marine origin.

The Miocene sediments beneath the Izumo-Matsue lowlands form a syncline buried beneath Quaternary sediments. Koura Formation is not exposed in the Matsue City area, and the Josoji, Ushikiri and Furue Formations occur only to the north of the city limits (Fig. 2). Shallower water or terrestrial equivalents of the latter three formations (Kawai-Kuri, Omori and Fujina, respectively) crop out in the south of Matsue City (Kano *et al.*, 1994; Fig. 2). The Furue and Fujina Formations are succeeded by the Matsue Formation, which outcrops in bluffs around the shores of Lake Shinji, and in hills within the city limits. Matsue Formation is dominated by pale sandstones and subordinate mudstones, but intercalated alkali basalt flows and associated volcanoclastic lithofacies also occur in its lower

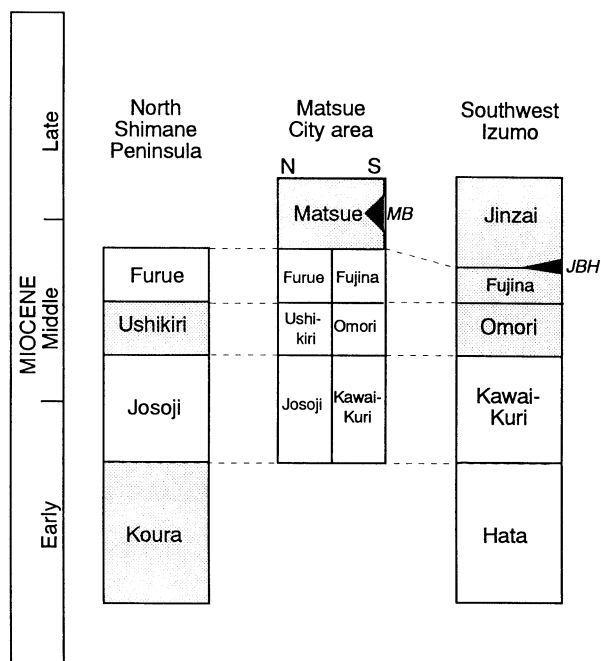


**Fig. 2.** Schematic stratigraphy and correlations between formations in Shimane Peninsula and the Matsue and Izumo districts. Shaded formations are those sampled in this study. Abbreviations: JBH – Jinzai Basalt Horizon; MB – Matsue Basalt. Based on Kano *et al.* (1989, 1991, 1994, 1997); EBGMS (1997) and Yamauchi (*pers. comm.* 2001)

and middle parts. The age of Matsue Formation is constrained in part by the basalts, the dates of which average 11 Ma (Morris and Itaya, 1997). From its lithofacies and faunal assemblages, Matsue Formation was deposited in a very shallow brackish to marine environment in a sheltered embayment (Nakayama *et al.*, 1996).

Early Miocene andesitic to dacitic lavas and pyroclastics of the Hata Formation occur southwest of Izumo, but lie outside our present study area. They are succeeded by sandstone, conglomerate, and andesitic to rhyolitic volcanic rocks of the Kawai and Kuri Formations, which are time equivalents of the Josoji Formation in Shimane Peninsula. Radiometric ages for Kawai volcanic rocks in the Iwami-Oda district to the west range between 15 and 18 Ma (Kano *et al.*, 1997). The Kawai Formation is non-marine to shallow marine, and the Kuri Formation marine (Kano *et al.*, 1997). Kawai-Kuri rocks occur near the southern edge of our study area in the Izumo district, but were not sampled. The middle Miocene Omori Formation overlies all three of the above units. It consists of volcanoclastic sandstones, mudstones, and debris flow deposits, along with massive and autobrecciated andesitic to dacitic lavas and associated pyroclastic deposits. Depositional environments of the sediments range from non-marine to shallow marine, including beach deposits. Detailed lithofacies analysis has been made in the area south of Lake Jinzai (Morita and Nakayama, 1999). Radiometric ages of the volcanic rocks range between 13 and 15 Ma (Kano *et al.*, 1997).

The Omori Formation is succeeded by onlapping sandstones, mudstones and lesser pebble conglomerates of the Fujina Formation (Kano *et al.*, 1997). Lithofacies are indicative of deposition in foreshore and shoreface environments (Morita and Nakayama, 1999). Fujina Formation grades upward into the Jinzai Formation, the equivalent of the Matsue Formation in this area.

The Jinzai Formation south of Lake Jinzai is distinguished by the presence of a small submarine alkali basalt tuff cone, the Jinzai Basalt. This has been described in detail by Kano (1998). The cone was constructed in relatively shallow water (50–150 m) by phreatomagmatic eruptions that produced hyaloclastites, bedded lapillistones and lapilli tuffs. These lithotypes pass laterally and vertically into bedded sandstone, mudstone and lesser conglomerate. Lithofacies analysis of this part of the succession suggests deposition mainly took place in lower shoreface to shelf settings (Morita and Nakayama, 1999), in slightly deeper water than Matsue Formation equivalents. The occurrence of storm deposits and their characteristic sedimentary structures in the Jinzai Formation (Morita and Nakayama, 1999) also suggests that its depositional environment was an open ocean coast. This is in contrast to the protected embayment in which the Matsue Formation in Matsue City was deposited.

In the latest 1:200,00 scale regional geologic map (EBGMS, 1997), Jinzai Formation in the Izumo area has been mapped as Matsue Formation, as occurs around Matsue City. Although the general appearance of the sandstones in both formations is similar, lithofacies and age differ between the two areas. The Jinzai Basalt has been K/Ar dated at  $13.2 \pm 0.6$  Ma (Takayasu and Sawada, 1989), which slightly overlaps the 13–15 Ma range of volcanic rocks in the Omori Formation (Kano *et al.*, 1997). This suggests that deposition of the Jinzai Formation in the Lake Jinzai area began somewhat earlier than did the Matsue Formation in its type locality (Fig. 2).

### Sample Suites

The samples in this study comprise three discrete sets (Fig. 1).

(1): A collection of 67 outcrop samples from the Omori, Fujina and Jinzai Formations in two areas southwest of Izumo City and southeast of Lake Jinzai. Morita and Nakayama (1999) have already reported a detailed lithofacies study of the area south of Lake Jinzai. The purpose of this collection was to establish the broad compositional ranges in each formation in this area and to examine their geochemical provenance signatures (Tateishi, *in prep.*) as a basis for comparison elsewhere in the district.

Samples from the Omori Formation include massive or brecciated calcalkaline subaerial dacitic lavas, a clast from a debris flow, and intercalated and overlying volcanoclastic sandstones and mudstones. Six of the twelve Omori

**Table 1:** Whole-rock XRF analyses of sedimentary and volcanic rocks from the Jinzai, Fujina and Omori Formations, Izumo district (hydrous basis). Major elements wt%, trace elements ppm. Column headings and codes are detailed in the footnotes to this table.

SANR	LOC	L/F	Lith1	Lith2	SiO <sub>2</sub>	TiO <sub>2</sub>	Al <sub>2</sub> O <sub>3</sub>	Fe <sub>2</sub> O <sub>3</sub>	MnO	MgO	CaO	Na <sub>2</sub> O	K <sub>2</sub> O	P <sub>2</sub> O <sub>5</sub>	LOI	Total	Ba	Ce	Cr	Ga	Nb	Ni	Pb	Rb	Sc	Sr	Th	V	Y	Zr		
<b>A. Southwest Izumo near Lake Jinzai</b>																																
<b>Jinzai Formation NW of Jinzai Basalt</b>																																
S-16/2	4	F-7	S	VFS	77.27	0.42	11.99	1.66	0.01	0.63	0.70	1.65	2.62	0.01	2.60	99.58	601	43	32	13	9	9	17	96	6.5	291	2.5	138	34	166		
S-17	4	F-7	M	MST	64.78	0.81	18.88	2.89	0.02	1.76	0.45	1.01	2.78	0.03	5.73	99.15	373	83	171	25	16	42	20	125	16.5	184	4.4	384	66	175		
S-18	4	F-7	M	MST-s	75.90	0.40	12.89	1.62	0.01	0.79	0.67	1.62	2.92	0.01	2.83	99.66	621	47	23	14	8	14	19	102	6.7	294	2.4	124	39	107		
S-19	4	F-7	M	MST	63.36	0.81	17.36	4.85	0.02	1.81	0.29	0.87	2.74	0.05	7.07	99.21	368	140	76	23	17	55	31	133	13.7	102	4.3	361	85	196		
S-20	5	F-5	S	FS	80.13	0.25	9.45	1.33	0.01	0.80	0.74	1.47	2.35	0.01	3.33	99.88	523	27	14	10	6	12	14	81	1.6	203	1.9	88	31	70		
S-63	20	F-2/3	S	FS	83.32	0.25	9.15	1.43	0.03	0.35	0.46	1.26	2.27	0.01	1.76	100.28	498	31	18	10	5	8	15	80	3.3	164	4.3	24	12	101		
S-64	20	F-2/3	S	MS-FS	84.07	0.37	8.57	1.57	0.02	0.38	0.47	1.10	1.89	0.01	1.78	100.23	450	38	34	9	6	8	13	68	4.7	148	4.6	35	10	156		
S-65	20	F-7	S	FS-m	62.23	0.98	18.01	6.78	0.04	1.68	0.59	0.81	1.26	0.04	6.65	99.07	247	57	33	20	8	17	17	49	24.3	116	6.3	196	24	174		
S-66	21	F-7	S	VFS-m	68.88	0.83	17.23	3.52	0.02	0.65	0.22	0.71	1.70	0.04	5.60	99.40	304	51	44	20	9	12	19	71	16.9	70	8.6	123	17	221		
S-67	22	F-7	S	VFS	77.36	0.53	11.39	2.00	0.02	0.68	0.66	1.75	2.59	0.03	2.52	99.53	496	61	48	14	10	14	15	96	5.4	236	7.3	61	14	305		
<b>Jinzai Formation, Jinzai Basalt horizon</b>																																
S-21	6	F-1	M	ZST	62.74	1.20	13.21	4.99	0.04	3.10	3.63	1.79	2.78	0.59	5.17	99.24	693	196	90	16	14	35	15	82	12.7	313	5.5	401	40	289		
S-22	6	F-1	M	ZST	48.16	1.86	14.06	8.17	0.05	6.86	7.09	0.84	1.54	1.20	9.59	99.41	961	323	117	19	20	40	15	69	17.4	507	8.6	594	39	288		
S-23	7	F-1	B	BBREC	54.26	1.12	15.45	7.31	0.10	5.53	7.24	2.16	1.77	0.44	4.22	99.59	477	125	106	18	11	48	13	45	21.8	732	4.3	522	28	128		
S-24	7	F-1	B	BBREC	52.69	1.15	15.41	7.42	0.08	6.29	7.84	1.91	1.71	0.54	4.55	99.59	658	130	112	17	11	52	15	44	21.7	740	4.5	530	26	115		
S-25	7	F-1	S	VCS	77.34	0.52	12.34	1.86	0.02	0.52	0.71	1.49	2.06	0.01	3.06	99.92	396	18	16	12	5	1	15	75	10.9	161	1.7	180	25	82		
S-32	11	F-1	S	VCS	53.23	0.92	15.62	8.29	0.07	7.87	5.89	1.47	1.22	0.16	4.76	99.50	730	27	169	11	9	93	14	40	24.7	252	2.4	499	26	94		
<b>Fujina Formation</b>																																
S-15	3	F-3	S	VFS-FS	61.48	0.74	16.16	6.54	0.06	3.04	4.47	2.43	1.19	0.12	3.36	99.61	352	44	4	17	7	5	16	32	18.6	287	2.2	337	32	115		
S-16	3	F-3	S	FS	54.16	0.88	12.69	6.76	0.60	1.83	11.85	2.37	1.19	0.08	7.82	100.23	254	31	18	13	5	8	10	35	21.3	213	2.0	474	29	127		
S-26	8	F-3	S	FS	73.12	0.37	13.80	3.36	0.03	0.92	1.46	1.84	2.39	0.01	2.54	99.85	558	30	12	13	5	13	16	87	8.2	326	1.9	160	47	69		
S-27	8	F-4	S	FS	79.47	0.25	10.76	2.30	0.02	0.49	0.96	1.78	1.93	0.02	2.01	99.99	387	20	11	11	3	3	11	64	8.4	165	3.0	46	16	77		
S-28	8	F-4	S	VFS-m	64.81	0.51	15.70	5.91	0.02	1.75	0.75	1.03	2.22	0.01	6.75	99.45	418	30	25	20	7	16	10	100	17.8	139	2.3	457	44	129		
S-29	8	F-4	S	VFS	63.50	0.84	17.36	5.43	0.02	1.42	2.56	1.95	1.47	0.03	4.95	99.52	469	63	28	17	6	10	16	63	17.3	246	2.6	501	40	109		
S-33	12	F-2	S	VFS-FS	71.55	0.65	14.63	2.60	0.01	0.89	0.47	1.18	2.49	0.05	4.90	99.43	403	79	50	16	9	14	16	88	10.8	150	7.8	117	23	233		
S-34	12	F-4	M	MST	61.50	0.79	20.64	3.17	0.01	1.47	0.13	0.45	2.48	0.02	8.38	99.03	283	85	57	23	14	14	17	102	21.3	61	10.6	152	36	172		
S-35	12	F-4	M	MST	63.85	0.78	18.40	3.38	0.01	1.46	0.28	0.71	2.90	0.02	7.33	99.14	361	81	66	23	15	29	13	121	18.2	83	12.8	136	29	192		
S-36	12	F-4	S	FS	77.50	0.48	12.19	1.79	0.01	0.60	0.30	1.17	2.57	0.01	3.35	99.98	503	60	34	14	8	15	14	89	10.2	111	6.5	72	15	167		
S-37	12	F-4	S	FS-m	74.43	0.64	12.43	3.07	0.02	0.95	0.46	1.16	2.55	0.03	3.78	99.52	419	57	43	16	10	13	14	99	12.8	134	7.5	113	16	203		
S-38	12	F-4	S	VFS	83.00	0.26	9.37	1.32	0.01	0.29	0.26	0.96	2.46	0.01	2.07	100.01	577	28	13	10	5	7	15	80	4.3	111	4.5	39	9	100		
S-44	17	F-5	S	VFS-FS	76.62	0.48	12.27	1.59	0.02	0.46	1.18	2.01	2.36	0.02	2.56	99.57	463	53	25	14	7	5	16	78	7.9	263	7.4	70	12	292		
S-45	17	F-5	M	MST	65.14	0.73	13.39	4.13	0.04	1.62	2.75	1.52	2.33	1.72	5.63	99.02	358	196	42	16	14	16	13	88	20.2	232	10.2	156	105	384		
<b>Omori Formation</b>																																
S-1	1	O-8	S	VCS	61.04	0.84	15.63	7.72	0.12	2.87	5.02	2.55	0.73	0.11	2.67	99.29	276	36	8	18	5	4	13	24	24.5	246	1.8	403	28	89		
S-2	1	O-8	M	MST	65.87	0.55	13.96	4.66	0.06	1.89	2.27	1.44	2.38	0.08	6.41	99.57	596	50	nd	15	8	4	20	105	12.0	172	3.3	147	55	165		
S-3	1	O-8	S	CS-VCS	59.58	0.67	16.91	6.37	0.10	2.09	5.44	2.48	1.80	0.20	3.60	99.25	443	57	3	18	6	3	16	58	16.5	331	2.4	269	48	94		
S-4	1	O-8	S	VCS	66.69	0.62	14.42	4.27	0.08	1.36	3.31	2.75	2.71	0.14	2.57	98.93	617	53	nd	15	7	2	20	88	13.3	239	3.1	200	59	137		
S-5	2	O-5	S	CS	59.59	1.19	16.54	8.89	0.11	2.14	5.24	2.50	0.58	0.17	2.80	99.74	336	31	4	19	6	3	9	22	38.1	303	1.4	722	41	75		
S-6	2	O-1	D	FLOW	68.44	0.72	14.17	5.25	0.14	1.09	4.19	3.52	1.44	0.21	0.81	99.96	321	33	4	15	5	1	10	43	20.3	222	1.6	138	42	94		
S-7	2	O-1	D	FLOW	68.67	0.71	14.16	4.98	0.14	1.04	4.17	3.66	1.39	0.20	0.62	99.75	318	24	nd	16	4	1	10	43	20.4	220	1.7	132	42	94		
S-8	2	O-1	D	FLOW	67.77	0.74	14.71	5.13	0.09	1.11	4.30	3.39	1.02	0.22	1.47	99.95	269	39	1	17	6	2	11	28	21.1	234	1.6	147	55	95		

**Table 1 (ctd)**

SANR	LOC	L/F	Lith1	Lith2	SiO <sub>2</sub>	TiO <sub>2</sub>	Al <sub>2</sub> O <sub>3</sub>	Fe <sub>2</sub> O <sub>3</sub>	MnO	MgO	CaO	Na <sub>2</sub> O	K <sub>2</sub> O	P <sub>2</sub> O <sub>5</sub>	LOI	Total	Ba	Ce	Cr	Ga	Nb	Ni	Pb	Rb	Sc	Sr	Th	V	Y	Zr		
<b>Omori Formation (ctd)</b>																																
S-9	2	O-5	D	CLAST	69.65	0.51	14.09	5.14	0.06	0.57	4.07	3.50	1.66	0.11	0.63	99.97	299	28	nd	15	4	2	10	65	16.7	205	1.4	215	41	85		
S-10	2	O-9	S	VCS	62.93	0.93	16.23	6.80	0.06	1.73	4.75	2.78	0.62	0.15	2.87	99.85	309	29	8	18	5	4	11	21	28.7	321	1.8	402	47	84		
S-11	2	O-9	S	VCS	62.07	1.04	19.44	5.54	0.03	1.52	1.42	1.19	0.60	0.01	6.88	99.74	611	6	5	22	5	5	14	23	32.1	177	1.7	464	26	116		
S-12	2	O-9	S	VFS-FS	69.50	0.58	14.49	3.50	0.03	1.16	2.86	2.40	2.22	0.04	3.00	99.77	459	42	14	16	6	7	16	67	14.1	403	2.1	274	43	172		
S-13	2	O-9	S	VFS-FS	68.85	0.54	14.04	3.99	0.03	1.87	2.18	2.14	2.22	0.03	3.89	99.79	444	35	16	15	6	4	12	69	12.4	352	2.1	247	33	143		
S-30	9	O-9	S	VFS	58.03	1.85	11.62	13.76	0.08	4.07	3.07	1.85	1.34	0.12	3.00	98.79	374	32	64	13	8	14	15	54	33.7	249	2.7	1104	31	144		
S-31	10	O-9	S	VCS	61.07	0.56	15.98	5.21	0.08	2.28	4.01	1.63	1.76	0.10	6.87	99.55	577	40	10	15	6	6	13	82	12.8	523	2.3	265	50	68		
S-39	13	O-1	D	FLOW	70.37	0.53	13.84	4.57	0.07	0.35	4.16	3.61	1.38	0.12	0.69	99.70	313	34	3	16	5	nd	13	37	14.8	274	3.2	60	22	131		
S-40	14	O-1	D	FLOW	67.31	0.85	16.61	3.63	0.04	0.36	4.99	4.03	1.33	0.17	0.45	99.77	269	41	nd	20	5	nd	11	34	22.6	337	4.0	80	32	132		
S-41	15	O-10	M	FLOW	52.89	1.14	18.13	6.24	0.03	3.86	0.91	0.21	1.12	0.03	14.58	99.13	625	57	nd	26	6	11	13	20	23.7	703	4.5	105	44	126		
S-42	16	O-11	S	VFS	66.56	0.57	15.99	3.20	0.03	1.35	1.21	2.20	2.71	0.04	5.29	99.16	384	46	11	19	8	11	22	87	12.9	393	8.0	83	23	165		
S-43	16	O-11	S	VFS-FS	67.21	0.57	16.17	2.52	0.03	1.23	1.61	2.50	2.68	0.08	4.76	99.37	405	138	10	19	13	12	21	89	11.3	386	8.1	84	111	165		
<b>(B)Fujina Formation, South Nishi-Izumo</b>																																
S-46	18	B-1	S	MS-VCS	71.73	0.43	12.94	2.66	0.02	0.59	2.55	2.29	2.17	0.06	4.25	99.69	652	22	14	14	5	3	13	71	11.2	625	3.9	69	13	97		
S-47	18	B-1	S	VFS-m	69.71	0.62	13.54	3.30	0.02	1.11	1.13	1.66	2.19	0.04	6.05	99.36	500	55	32	17	8	4	12	87	15.1	530	7.1	95	17	261		
S-48	18	B-1	M	MST	63.69	0.65	16.71	4.94	0.01	1.70	0.98	0.93	2.53	0.03	6.90	99.08	315	56	58	21	11	14	7	122	16.3	170	9.7	149	23	166		
S-49	18	B-2	S	FS-VFS	75.80	0.41	12.62	2.24	0.02	0.48	1.21	2.04	2.33	0.01	2.60	99.74	487	26	17	13	5	6	12	83	6.2	243	5.1	55	12	145		
S-50	19	B-2	M	MST	62.34	0.65	16.20	5.60	0.01	1.78	1.02	0.87	2.40	0.02	8.14	99.04	301	51	58	21	11	17	10	114	17.7	181	10.2	145	23	161		
S-51	19	B-2	S	FS-VFS	71.87	0.41	14.00	2.84	0.01	0.82	1.15	1.68	2.53	0.02	4.25	99.58	470	32	12	15	6	7	16	88	6.5	256	5.1	60	14	139		
S-52	19	B-2	M	MST	62.21	0.64	16.62	5.77	0.01	1.86	1.04	0.83	2.36	0.04	7.67	99.06	267	56	56	22	10	20	13	114	14.4	174	10.1	153	29	157		
S-53	19	B-2	S	MS-FS	72.72	0.41	13.37	2.86	0.01	0.77	1.08	1.73	2.52	0.02	3.97	99.45	445	28	15	14	6	8	13	90	8.9	220	5.3	62	12	162		
S-54	19	B-3	S	FS-VFS	74.50	0.65	12.13	3.10	0.03	0.82	1.32	1.83	2.32	0.04	2.86	99.59	416	58	25	13	8	11	15	80	8.6	222	8.3	97	17	371		
S-55	19	B-3	M	MST	61.25	0.63	16.56	4.48	0.01	1.55	1.67	1.06	1.74	0.03	10.30	99.29	273	36	11	21	5	7	11	54	23.5	275	5.8	127	18	161		
S-56	19	B-3	S	FS	75.57	0.65	12.40	2.61	0.02	0.89	0.53	1.25	2.08	0.01	3.66	99.68	398	48	22	14	7	5	13	72	11.1	149	5.8	100	16	295		
S-57	19	B-3	S	FS-VFS	73.03	0.52	13.30	2.55	0.02	0.84	1.49	2.28	2.02	0.02	4.69	99.57	532	60	26	15	6	9	15	79	8.1	300	6.1	72	22	219		
S-58	19	B-4	S	CS-VCS	77.93	0.24	11.74	1.79	0.01	0.37	0.81	1.79	2.23	0.01	2.90	99.82	428	28	14	12	5	9	13	85	8.0	149	3.8	33	24	81		
S-59	19	B-4	S	MS-CS	76.28	0.37	12.15	1.78	0.03	0.35	0.98	1.98	2.37	0.01	3.13	99.44	458	23	7	13	4	7	15	88	7.6	191	4.2	51	14	84		
S-60	19	B-5	M	MST	64.39	0.69	14.91	4.93	0.02	1.82	0.54	1.02	2.54	0.05	8.10	99.00	321	72	62	20	12	19	18	118	16.8	159	11.4	140	23	175		
S-61	19	B-5	S	VFS	74.81	0.66	11.51	2.71	0.02	0.91	1.13	1.49	2.28	0.04	3.90	99.46	463	60	42	13	7	8	15	82	10.0	436	7.3	100	16	359		
S-62	19	B-5	S	VFS	74.66	0.58	13.66	2.35	0.02	0.64	0.33	1.36	2.44	0.01	3.47	99.52	405	54	27	15	7	6	11	85	9.0	88	6.7	79	14	304		

**NOTES:** Column headings: SANR = Sample number; LOC=location, numbers as in Fig. 2; L/F=Lithofacies code ; LITH1=broad lithotype; LITH2=texture (visual estimates); LOI=loss on ignition.

Codes: L/F: (A) Southwest Izumo near Lake Jinzai: Lithofacies codes after Morita & Nakayama (1999) - *Jinzai and Fujina Formations*: F-1: basaltic lava and volcanic breccia (shallow marine); F-2: boulder cgl and very coarse sst (gravelly fluvial); F-3: sandstone and conglomerate (foreshore); F-4: fine sandstone (upper shoreface); F-5: fine and very fine sandstone (lower shoreface); F-7: sandy mudstone (shelf).  
*Omori Formation*: O-1: massive lava (terrestrial); O-5: boulder conglomerate (subaerial or subaqueous debris flow); O-8 sandstone and conglomerate, discoid gravels (foreshore); O-9: medium to fine sandstone (upper shoreface); O-10: medium to fine sandstone with mud drapes (upper shoreface); O-11: fine and very fine massive sandstone (lower shoreface).  
 (B) South Nishi-Izumo: B-1: sst + cgl gravel dune (lwr shoreface +gravelly fluvial inflow); B-2 sst + cgl (lwr shoreface + gravelly fluvial inflow); B-3: sst + mnr cgl (upper shoreface); B-4: sst (erosional surface and delta front); B-5: sst and mst (tidal and intertidal deposits).  
 LITH1: S=sandstone; M=mudstone or siltstone; B=alkali basalt; D=Omori volcanics (dacitic).  
 LITH2: Sediments - VCS=very coarse sand to granule; CS=coarse sand; MS=medium sand; FS=fine sand; VFS=very fine sand; ZST=siltstone; MST=mudstone. Modifiers -s and -m are sandy and muddy, respectively. Volcanics - BBREC=basaltic breccia; FLOW=subaerial dacite; CLAST=clast in debris flow facies.  
 nd Not detected. Total Fe as Fe<sub>2</sub>O<sub>3</sub>.

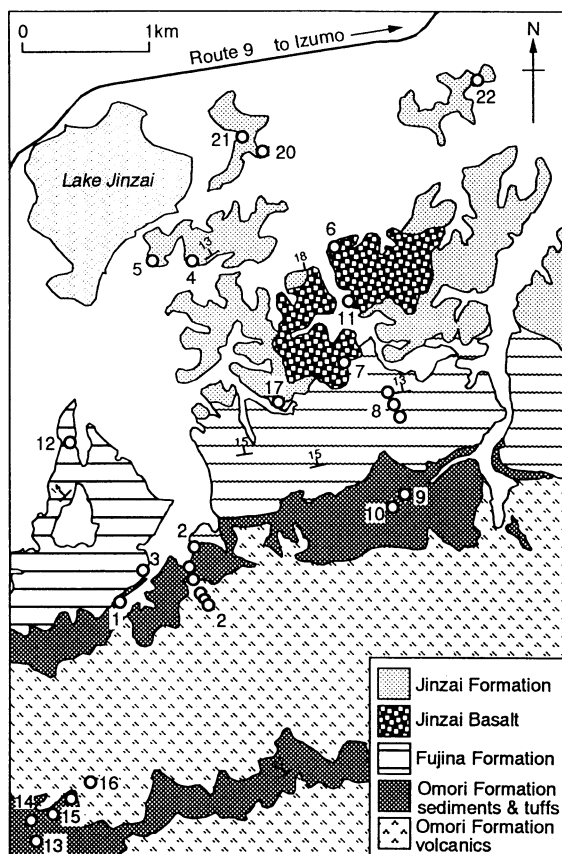


Fig. 3. Geology and sample localities in the area south of Lake Jinzai, Izumo district. Based on Kano *et al.* (1997) and Morita and Nakayama (1999).

lithofacies identified by Morita and Nakayama (1999) are represented in the collection (Table 1). Fourteen samples of Fujina Formation sediments (eleven sandstones, three mudstones) were collected from four localities (Fig. 3). The sandstones were all fine- or very fine-grained, and most were from lithofacies F-3 and F-4 (Morita and Nakayama, 1999), representing foreshore and upper shoreface environments.

Samples from the Jinzai Basalt horizon were collected at three localities (Fig. 3), and include basaltic breccia, very coarse-grained sandstones, and hyaloclastitic siltstones (Table 1). All belong to lithofacies F-1 (shallow marine basaltic lava and volcanic breccia) of Morita and Nakayama (1999). Ten samples (seven sandstones, three mudstones) were also collected from the Jinzai Formation from five localities stratigraphically above the Jinzai Basalt horizon (Fig. 3). The sandstones are typically very fine- to medium-grained, and most were deposited in a shelf environment.

Seventeen additional samples (12 sandstones, five mudstones) were collected from two continuous sections in South Nishi-Izumo, from an area mapped as Fujina Formation by Kano *et al.* (1997). The area is currently being mapped in detail by Bandou (*in prep.*). For convenience, we here informally assign lithofacies in the

area to five groups, denoted B-1 to B-5 (Table 3 B). These represent lower shoreface with gravelly fluvial inflow (B-1 and B-2), upper shoreface (B-3), delta front (B-4) and tidal and intertidal deposits (B-5). The sandstones analysed here span a range in texture from very fine sand through to very coarse sand.

(2): A suite of 53 Matsue Formation sandstones and mudstones taken from a 110 m drillcore put down by Shimada Technical Consultants Ltd. The hole was located near the northern shore of Lake Shinji in Sada-cho, Nishihama, Matsue City, at 35° 28' 22.4" N, 133° 00' 38.0" E. The hole penetrated 110 m of poorly consolidated sediments which were dominated by relatively monotonous pale cream/buff, grey or orange fine- or very fine-grained sandstone. Occasional thin horizons of coarser sand or mud occurred sporadically throughout the core. A single coarse sand unit at 72.10–75.90 m BCL that contains subrounded basaltic andesite pebbles is interpreted as a debris flow deposit. At the base of the core (107.7–110.0 m BCL), the dominant sandstone lithofacies gave way to thinly bedded (1–2 cm) lenticular fine sand and mud alternations. Apart from these two intervals, the lithofacies observed are very similar to those exposed in cliff outcrops in the immediate area. Stratigraphically, the core intersects the lower part of the Matsue Formation, and thus predates the alkalic volcanism that occurred around 11.0 Ma (Morris and Itaya, 1997).

(3): Assorted outcrop samples collected from the Matsue City area and the northern coast of Shimane Peninsula. Three samples (AH 1–3; Table 3) were collected from the westernmost outcrop of Matsue Formation on the north shore of Lake Shinji in Asahi-cho (Fig. 1). These are from the base of the Matsue Formation, and consist of two very fine-grained sandstones and an entrained clast of Furue Formation mudstone. Five samples were collected from the lower middle of the Matsue Formation at Nanpeidai (Fig. 1, Table 3). These consist of mildly weathered subaerial Matsue Basalt (NPD 5), the highly weathered top of the flow (NPD 1), and three overlying very shallow marine sandstones (NPD 2–4). The basaltic samples were collected to provide some measure of the composition of any basalt or basaltic weathering products that could be supplied to the sediments. Eight sandstones and mudstones (KU 1–8) were also collected from a former quarry site nearby. This locality has been described in detail by Nakayama *et al.* (1996) and Nakayama (1997).

A small suite of turbidite sandstones and mudstones of the Ushikiri Formation were collected as a pilot study. Five samples (US 4 A–6) were collected from thin (<20 cm) sand-dominated  $T_{b-e}$  and  $T_{c-e}$  turbidites exposed on the shore platform on the Chikumi coast. Stratigraphically, these samples lie near the base of the Ushikiri Formation, 10–50 m above the contact with the underlying Josoji Formation.

Three green volcanoclastic sandstones (KO 1, 2, and 4) and an interbedded tuff (KO 3) were collected from an

exposure of the Koura Formation on the east side of the bay at Karuba (Fig. 1). Coarse to fine-grained sandstones occur there in fining-upward fluvial cycles, and contain numerous interbedded tuffs 0.4-5.0 m thick. An additional Koura sandstone and an andesite (KO 6, 5) were also taken from a quarry and road section on the southern side of the peninsula opposite Mihonoseki.

### Analytical Methods

All indurated samples were manually chipped to remove deleterious material such as veins or weathering rinds. A number of weakly lithified sandstone samples from the Matsue, Omori, Jinzai and Fujina Formations had suffered slight to moderate pervasive weathering, and complete removal of weathered grains was not possible. For the collection from the Izumo district (Table 1), outermost surfaces and clots of weathering products were removed as far as was practical. This procedure was not followed in the case of the Matsue Formation drillcore (Table 2). Pervasively weathered and fresh intervals persisted throughout the core, and bulk samples were taken to permit future tests of the effects of such alteration on conventional weathering indices, and to determine if immobile element ratios had been affected. Prepared material of both indurated and unconsolidated samples was repeatedly washed in deionised distilled water before drying at 110°C prior to crushing.

The majority of the samples were crushed in a tungsten carbide ring mill for 30-45 seconds (Roser *et al.*, 1998). Sample weights were typically 75-150 g. However, all samples from the Matsue Formation drillcore (Table 2) were ground in an automatic pestle and mortar for 60 minutes each, in sample aliquots of 20 g. This permitted cobalt analyses to be made in this suite. After crushing, 10 g subsamples were dried for at least 24 h at 110°C prior to conventional gravimetric determination of loss on ignition (LOI) by ignition at 1000°C for 2 h. The ignited material from the LOI determinations was retained, disaggregated in an agate pestle and mortar, and returned to a 110°C oven for a further 24 hours. Fusion beads for X-ray fluorescence analysis (XRF) were then prepared from this material (ignited basis).

All analyses contained in this report were carried out in the Department of Geoscience, Shimane University, using a Rigaku RIX-2000 spectrometer equipped with a Rh-anode X-ray tube. The analyses were accumulated between 1996 and 2001, using two different methods. Major and trace element analyses of the samples in Tables 2 and 3 were originally made in 1996-7 using fusion beads prepared with lithium tetraborate flux using a 1:5 sample to flux ratio, after the method of Norrish and Hutton (1969). This technique was abandoned in 1998 in favour of the method of Kimura and Yamada (1966). That method uses fusion beads prepared with an alkali flux comprising 80% lithium

tetraborate and 20% lithium metaborate, with a sample to flux ratio of 1:2. Both major and 14 trace elements are determined from the same fusion beads. The lower dilution used gives higher count rates and improved peak/background ratios, and consequently lower limits of detection and greater precision than does the 1:5 method.

### Results and Discussion

Hydrous analytical data for the three suites are given in Table 1 (Izumo district), Table 2 (Matsue Formation drillcore) and Table 3 (Matsue Formation outcrop samples, and Ushikiri and Koura Formations, Shimane Peninsula). All data in Table 1 were determined in 2001, using the 1:2 method described above. Data in Tables 2 and 3 are a combination of 1:2 and 1:5 data. Although all these samples were originally analyzed using the 1:5 technique, they were subsequently reanalyzed for most trace elements using new 1:2 fusion beads, to take advantage of the superior precision the 1:2 method offers, and to add Sc analyses. However, data listed for As, Co and Zn in Tables 2 and 3 are the original 1:5 data, as these elements are not included in the current 1:2 calibration. The yttrium values listed in all tables have also been corrected for the methodological bias discussed by Roser *et al.* (2000), and consequently are comparable with results obtained by ICP-MS.

Elemental compositions of individual samples and formations can be conveniently compared using normalised multi-element diagrams (spidergrams). The normalizer used here is the Upper Continental Crust (UCC) estimate of Taylor and McLennan (1985). Both sample compositions and UCC were first recalculated to 100% volatile-free prior to normalization. Elements are plotted left to right in the order of progressive depletion or enrichment relative to UCC in the average Cenozoic greywacke of Condie (1993), following Dinelli *et al.* (1999). Using this order, many incompatible elements (e.g. Nb, K, Zr, Sr) plot at left, and most compatible elements (e.g. Sc, Fe, Ti, Ni, Cr, and V) lie to the right (Fig. 4).

Typical patterns of common source lithotypes are given in Fig. 4, using published average rock compositions. Published averages were used here because although some analyses of potential source rocks in the district are available in the literature, none contain comprehensive trace element analyses. Relatively mafic source rocks (e.g. basalts, andesites) have patterns which generally increase from normalized abundances <UCC at left, to >UCC at right (Fig. 4a), whereas felsic volcanic rocks tend to have normalised abundances similar to or less than UCC. For felsic volcanics, depletion relative to UCC is especially marked for the segment Fe-V (Fig. 4b). Similar patterns are also shown by average felsic plutonic rocks (Fig. 4b). Plutonic rocks form a substantial part of the Chugoku Mt. hinterland of the study area (Fig. 1), and thus could have supplied detritus to the Miocene successions analysed here.

Whole-rock geochemical compositions of Miocene sedimentary and volcanic rocks  
from the Izumo–Matsue districts and Shimane Peninsula, SW Japan

Table 2: Whole-rock XRF analyses of Matsue Formation sandstones and mudrocks, Shimada Consultants Ltd drillcore, Nishihama Sada-cho, Matsue City. Major elements wt%, trace elements ppm.

Sample	Interval m	Lith	Wea	SiO <sub>2</sub>	TiO <sub>2</sub>	Al <sub>2</sub> O <sub>3</sub>	Fe <sub>2</sub> O <sub>3</sub> T	MnO	MgO	CaO	Na <sub>2</sub> O	K <sub>2</sub> O	P <sub>2</sub> O <sub>5</sub>	LOI	Total	As	Ba	Ce	Co	Cr	Ga	Nb	Ni	Pb	Fb	Sc	Sr	Th	V	Y	Zn	Zr	
MF1	0.80 - 0.90	MS	MP	78.73	0.23	12.10	1.38	0.02	0.02	0.18	0.78	2.84	0.01	3.09	99.84	1	546	19	14	12	13	7	9	14	100	3.7	86	5.0	29	12	33	95	
MF2	2.60 - 2.70	FS	MP	77.54	0.25	12.09	1.58	0.02	0.32	0.25	1.02	3.17	0.01	3.09	99.35	2	546	21	9	14	12	13	7	14	100	4.7	107	4.7	37	14	38	98	
MF3	5.60 - 5.65	VFS	MP	75.46	0.44	13.08	2.10	0.01	0.61	0.30	1.40	3.03	0.01	2.55	90.38	3	485	30	13	29	15	6	19	18	85	8.5	221	6.5	61	17	76	224	
MF4	5.75 - 5.85	VFS	MP	80.51	0.30	9.99	1.42	0.01	0.36	0.74	1.29	2.60	0.01	2.55	99.77	3	495	39	11	25	11	6	12	14	77	5.7	218	4.0	40	14	33	144	
MF5	7.70 - 7.80	FS	MP	80.01	0.30	10.16	1.46	0.02	0.43	0.94	1.32	2.84	0.01	2.85	100.15	3	502	44	12	21	11	6	13	14	80	5.5	209	4.1	43	16	38	146	
MF6	10.80 - 10.90	FS	MP	80.05	0.25	9.99	1.35	0.02	0.35	0.96	1.33	2.80	0.01	2.85	99.84	7	528	44	10	15	11	6	13	14	80	5.5	209	4.1	43	16	38	146	
MF7	13.50 - 13.60	VFS	MP	79.76	0.24	10.47	1.56	0.01	0.28	0.90	1.18	2.84	0.01	2.89	100.25	5	506	26	10	12	12	6	12	15	87	5.2	183	4.3	35	13	33	88	
MF8	15.90 - 16.00	VFS	U	81.38	0.17	8.72	0.96	0.01	0.33	0.82	1.12	2.58	0.01	3.75	99.81	5	490	20	9	15	9	6	11	12	76	3.6	187	2.2	23	11	21	74	
MF9	16.60 - 16.70	VFS	SW	82.55	0.17	8.80	1.20	0.01	0.30	0.86	1.09	2.62	0.01	3.01	100.61	4	477	19	10	11	8	6	11	78	3.6	191	2.4	22	10	24	75		
MF10	18.30 - 18.40	VFS	U	81.56	0.16	8.68	1.07	0.01	0.32	0.84	1.09	2.55	0.01	3.01	100.31	3	464	19	10	11	9	6	11	10	75	4.0	207	2.3	18	11	24	74	
MF11	19.60 - 19.70	VFS	U	82.63	0.20	8.93	1.27	0.01	0.34	0.85	1.09	2.53	0.01	2.62	100.48	3	476	26	11	12	9	6	14	13	75	3.9	208	2.6	29	12	29	83	
MF12	20.90 - 21.00	VFS	SW	81.42	0.18	9.54	1.48	0.01	0.32	0.78	1.11	2.72	0.01	2.49	100.26	10	518	17	9	15	10	5	11	12	80	2.7	209	2.7	21	10	23	79	
MF13	23.70 - 24.80	FS	SW	81.87	0.19	9.50	1.86	0.02	0.36	0.65	1.05	2.63	0.01	2.21	100.34	12	540	26	14	15	11	5	12	14	80	1.6	159	3.3	25	12	23	81	
MF14	24.60 - 24.90	FS	VSW	81.98	0.16	9.42	1.82	0.01	0.34	0.63	0.97	2.61	0.01	2.18	100.17	15	515	24	12	14	11	7	9	12	79	3.2	158	2.9	30	11	23	78	
MF15	25.90 - 26.60	FS	U	82.68	0.17	9.17	1.39	0.01	0.37	0.54	0.98	2.65	0.01	2.50	100.39	7	483	19	11	12	11	6	12	13	77	2.3	128	2.8	23	11	19	78	
MF16	28.40 - 28.50	FS	U	81.69	0.15	8.69	1.44	0.02	0.32	0.92	1.16	2.66	0.01	2.97	100.02	3	501	19	11	16	12	8	5	9	12	70	2.6	242	2.2	19	11	21	75
MF17	30.50 - 30.60	FS	U	82.62	0.20	9.01	1.65	0.02	0.48	0.60	0.99	2.53	0.01	2.66	100.57	3	472	19	11	16	12	7	10	12	70	2.6	191	3.5	29	11	28	86	
MF18	34.30 - 34.40	FS	SP	74.49	0.31	11.20	3.42	0.03	0.93	0.73	1.07	2.58	0.02	3.57	100.14	6	545	28	15	19	14	8	13	15	62	6.2	145	3.9	36	16	43	108	
MF19	35.80 - 35.90	VFS	SP	80.04	0.21	9.40	2.13	0.02	0.68	0.55	0.98	2.37	0.01	3.67	100.07	4	506	21	13	13	13	7	10	13	74	4.0	128	2.0	33	12	27	79	
MF20	37.30 - 37.40	VFS	U	82.91	0.16	8.54	1.56	0.02	0.58	0.41	0.97	2.37	0.01	2.45	99.99	3	469	19	11	10	10	6	8	12	72	3.3	97	2.0	20	11	23	76	
MF21	40.85 - 40.95	FS	U	82.60	0.17	9.00	1.63	0.02	0.64	0.48	0.97	2.43	0.01	2.30	100.25	4	453	16	12	11	11	7	8	12	75	3.1	96	2.7	25	11	28	78	
MF22	44.00 - 44.10	FS	SP	82.29	0.17	8.66	1.84	0.02	0.64	0.45	0.92	2.34	0.01	2.59	99.92	3	453	20	11	16	11	7	12	12	71	4.0	91	1.9	24	11	22	79	
MF23	44.70 - 44.80	MST	U	68.73	0.49	13.16	5.17	0.04	1.24	0.79	1.05	2.37	0.03	3.71	100.19	8	432	58	22	37	17	10	20	20	89	11.1	119	6.6	79	23	70	168	
MF24	46.75 - 46.85	FS	U	83.35	0.17	8.38	1.48	0.02	0.51	0.57	1.02	2.25	0.03	3.32	101.10	3	471	5	11	11	10	6	9	11	68	3.3	127	2.0	23	11	25	72	
MF25	49.70 - 49.80	FS	SP	82.59	0.17	8.89	1.49	0.02	0.48	0.80	1.05	2.41	0.02	2.36	100.28	3	486	17	11	13	9	6	8	12	74	3.9	207	2.7	23	11	25	78	
MF26	51.45 - 51.55	FS	SP	82.68	0.17	8.55	1.46	0.02	0.47	0.78	1.00	2.30	0.02	3.31	99.75	4	508	22	10	12	9	7	8	10	70	4.9	201	1.7	26	11	25	78	
MF27	52.30 - 52.40	MST	U	70.91	0.45	11.92	5.01	0.03	1.09	0.86	1.04	2.27	0.03	6.70	100.31	5	444	50	18	37	15	9	18	16	84	8.0	138	6.8	86	21	62	166	
MF28	55.60 - 55.70	FS	U	81.77	0.19	8.87	1.88	0.02	0.73	0.50	0.93	2.31	0.02	2.75	99.94	4	439	23	12	14	11	10	12	71	4.0	91	2.6	25	12	23	86	94	
MF29	58.70 - 58.80	FS	U	82.18	0.17	8.92	1.83	0.02	0.56	0.79	0.96	2.39	0.09	2.32	100.19	3	512	27	12	13	10	6	9	12	74	4.3	149	2.9	25	12	27	79	
MF30	61.60 - 61.70	FS	U	81.99	0.16	8.46	1.48	0.02	0.55	0.64	1.12	2.43	0.02	3.07	99.93	2	471	21	10	13	10	5	9	12	73	2.6	145	2.3	26	10	24	81	
MF31	63.50 - 63.60	MS	SP	82.68	0.16	8.99	1.33	0.02	0.51	0.66	1.29	2.85	0.02	1.89	100.39	2	464	13	12	11	10	6	8	12	90	2.6	137	2.6	19	10	21	76	
MF32	66.80 - 66.90	MS	SP	81.46	0.15	8.82	1.06	0.02	0.45	0.64	1.36	2.85	0.01	2.41	99.34	2	445	13	10	11	9	6	7	11	83	2.5	141	2.3	17	10	19	73	
MF33	68.50 - 68.60	MS	SP	81.23	0.14	8.89	0.97	0.02	0.41	0.63	1.49	3.09	0.02	2.21	99.10	2	439	15	11	7	9	5	6	12	68	1.2	139	3.4	16	11	20	72	
MF34	70.90 - 71.00	MS	SP	82.04	0.15	8.85	0.97	0.02	0.44	0.63	1.52	3.03	0.02	1.49	99.17	2	444	17	11	13	9	5	6	12	68	3.6	147	3.0	17	11	18	69	
MF35	72.80 - 72.95	MST	U	69.31	0.46	12.93	9.31	0.04	1.50	1.00	1.19	2.24	0.06	11.49	100.43	13	348	52	18	38	16	9	15	16	86	9.6	110	6.7	77	25	70	141	
MF36	73.00 - 73.10	MST	U	69.31	0.46	12.93	9.31	0.04	1.50	1.00	1.19	2.24	0.06	11.49	100.43	13	348	52	18	38	16	9	15	16	86	9.6	110	6.7	77	25	70	141	
MF37	73.00 - 73.10	MS	U	81.54	0.15	8.62	0.98	0.02	0.36	0.85	1.57	2.86	0.02	2.33	99.80	2	436	50	14	39	15	9	17	11	83	10.2	103	6.0	79	25	65	134	
MF38	73.00 - 73.10	MS	U	81.54	0.15	8.62	0.98	0.02	0.36	0.85	1.57	2.86	0.02	2.33	99.80	2	436	50	14	39	15	9	17	11	83	10.2	103	6.0	79	25	65	134	
MF39	79.90 - 79.90	MST	U	64.44	0.65	13.32	5.35	0.04	1.70	1.16	1.35	2.90	0.05	8.49	99.84	15	378	77	23	53	18	14	24	19	97	11.3	155	8.1	117	25	89	235	
MF40	80.50 - 80.60	FS	U	80.41	0.20	11.59	3.42	0.02	0.75	1.06	1.72	3.03	0.05	3.26	100.08	16	502	31	18	10	15	8	10	20	95	4.8	165	5.6	39	14	25	97	
MF41	80.50 - 80.70	FS	U	80.41	0.20	9.07	1.93	0.02	0.55	1.01	1.49	2.39	0.03	2.95	100.03	8	502	27	13	16	9	6	10	13	73	3.8	283	3.0	32	11	21	83	
MF42	83.20 - 83.30	FS	SP	78.32	0.24	10.14	2.28	0.02	0.62	1.11	1.67	2.67	0.03	3.11	100.21	8	541	32	16	20	11	6	13	16	82	4.6	288	3.1	36	13	30	118	
MF43	85.30 - 85.40	FS	SP	79.15	0.26	9.79	2.13	0.02	0.56	1.09	1.77	2.99	0.04	2.70	100.11	6	508	35	14	23	10	7	11	16	79	5.6	270	4.4	37	13	29	116	
MF44	88.80 - 89.00	FS	SP	78.32	0.27	9.93	2.43	0.02																									

**Table 3.** Whole-rock XRF analyses of surface outcrop samples from (A) Matsue Formation, Matsue City and (B) Miscellaneous Miocene rocks, Shimane Peninsula.  
Major elements wt%, trace elements ppm.

**(A) Matsue Formation, Matsue City Area**

SANR	LITH	SiO <sub>2</sub>	TiO <sub>2</sub>	Al <sub>2</sub> O <sub>3</sub>	Fe <sub>2</sub> O <sub>3</sub> T	MnO	MgO	CaO	Na <sub>2</sub> O	K <sub>2</sub> O	P <sub>2</sub> O <sub>5</sub>	LOI	Total	As	Ba	Ce	Cr	Ga	Nb	Ni	Pb	Rb	Sc	Sr	Th	V	Y	Zn	Zr
<i>Nanpeidai, Matsue City</i>																													
NPD1	WBAS	42.82	3.69	28.45	11.60	0.04	0.66	0.06	0.15	0.10	0.11	12.03	99.72	-	200	131	173	39	41	138	143	5	39.4	11	14.2	366	20	-	512
NPD2	VFS	78.82	0.45	12.67	1.61	0.01	0.28	0.05	0.12	0.92	0.02	4.81	99.75	2	167	38	17	14	10	16	11	38	11.3	22	3.8	48	12	20	142
NPD3	VFS	82.09	0.20	10.83	1.22	0.01	0.27	0.05	0.11	0.89	0.02	4.06	99.74	3	147	16	9	10	9	8	6	33	3.3	21	3.5	24	10	13	75
NPD4	MS	77.80	0.29	12.66	2.10	0.01	0.24	0.03	0.11	1.49	0.01	4.69	99.42	4	185	24	16	13	10	10	16	56	8.5	20	6.8	44	9	16	98
NPD5	BAS	50.83	1.87	19.63	8.16	0.11	4.03	4.91	3.20	1.83	0.65	4.72	99.93	1	678	82	102	20	21	87	5	56	21.8	297	7.1	217	31	78	279
<i>Asahi-cho, shore of lake Shinji near base of Matsue Formation</i>																													
AH1*	MST-C	66.53	0.68	16.01	5.72	0.04	1.69	0.20	0.38	2.12	0.03	6.10	99.49	11	410	55	38	21	12	11	18	87	14.5	61	6.6	116	45	56	186
AH2	VFS	82.64	0.22	9.98	1.02	0.01	0.28	0.09	0.41	2.51	0.01	2.53	99.71	2	453	19	17	10	7	5	13	80	1.7	54	4.4	25	13	7	85
AH3	VFS	72.83	0.16	10.81	8.36	0.01	0.20	0.14	0.82	2.37	0.02	3.80	99.53	4	558	8	4	9	7	23	17	74	4.0	66	2.4	21	8	39	67
<i>Nanpeidai, Matsue City, locality of Nakayama et al. (1996).</i>																													
KU1	VFS	81.04	0.22	10.08	1.31	0.01	0.19	0.49	1.44	2.70	0.02	2.01	99.51	3	623	11	7	9	4	3	14	87	2.3	284	1.3	24	9	11	75
KU2	VFS-ZST	78.30	0.32	12.00	1.51	0.01	0.30	0.38	1.35	2.68	0.02	2.82	99.69	5	521	23	4	12	6	5	18	88	6.7	179	3.1	49	11	29	99
KU3	ZST	76.22	0.38	12.29	2.48	0.01	0.41	0.40	1.71	2.79	0.02	2.93	99.63	7	446	40	18	13	8	5	18	96	7.5	126	3.0	48	17	39	143
KU4	FS	77.97	0.28	11.95	1.07	0.01	0.31	0.69	1.82	3.12	0.02	2.58	99.83	4	561	24	9	12	0	6	15	110	4.5	741	2.6	33	13	20	95
KU5	FS	82.39	0.22	9.81	0.73	0.01	0.19	0.52	1.50	2.61	0.02	1.59	99.58	1	465	11	7	10	3	5	12	86	3.2	348	1.7	19	10	17	76
KU6	FS	82.27	0.20	9.81	0.83	0.03	0.19	0.45	1.43	2.64	0.02	1.69	99.55	2	458	10	2	9	2	5	12	90	3.9	429	2.1	19	10	22	74
KU7	MST	77.54	0.45	11.09	1.93	0.01	0.50	0.37	1.52	2.08	0.03	4.09	99.61	5	408	43	32	13	10	10	17	75	8.1	124	4.7	57	14	26	182
KU8	FS	77.94	0.16	7.63	8.14	0.01	0.14	0.21	1.01	2.04	0.10	2.32	99.68	5	585	13	12	6	6	4	11	67	2.5	100	3.3	15	10	12	78

\*clasts of Furue Formation mudstone within basal Matsue Formation.

**(B) Miscellaneous analyses of Miocene rocks, Shimane Peninsula**

SANR	LITH	SiO <sub>2</sub>	TiO <sub>2</sub>	Al <sub>2</sub> O <sub>3</sub>	Fe <sub>2</sub> O <sub>3</sub> T	MnO	MgO	CaO	Na <sub>2</sub> O	K <sub>2</sub> O	P <sub>2</sub> O <sub>5</sub>	LOI	Total	As	Ba	Ce	Cr	Ga	Nb	Ni	Pb	Rb	Sc	Sr	Th	V	Y	Zn	Zr
<i>Ushiki Formation, Chikumi shore platform</i>																													
US4A	ZST	78.19	0.35	8.26	4.27	0.03	1.95	0.23	1.06	1.17	0.04	3.95	99.49	-	239	30	43	10	8	17	8	57	8.7	67	5.5	62	13	-	75
US4B	ZST	77.16	0.38	8.92	4.56	0.03	2.01	0.28	1.16	1.34	0.06	3.66	99.55	-	280	31	45	11	9	20	4	65	6.4	69	5.5	75	15	-	83
US5A	MS	61.83	0.60	15.65	6.88	0.07	4.85	1.78	4.42	0.40	0.19	3.36	100.03	-	405	32	28	17	4	15	8	11	16.2	370	5.4	121	21	-	112
US5B	MS	55.44	0.75	17.97	7.93	0.10	5.55	2.78	4.34	0.55	0.23	4.10	99.73	-	455	25	49	19	6	17	11	18	22.4	369	5.2	153	20	-	104
US6	MS	67.42	0.50	12.65	5.51	0.07	4.15	1.92	3.76	0.32	0.13	3.24	99.67	-	300	30	14	13	7	8	5	10	10.6	343	4.5	85	17	-	114
X-US1	MS	77.27	0.24	12.38	1.54	0.03	0.39	0.32	4.86	2.09	0.06	0.92	100.10	-	529	36	2	9	7	5	4	57	5.6	156	8.0	17	22	-	163
<i>Koura Formation, east side of bay at Karuba, Mihonoseki</i>																													
KO1	MS	62.00	0.72	16.76	5.53	0.17	2.78	2.31	4.82	2.60	0.17	2.07	99.92	-	1040	58	20	19	9	11	7	46	14.1	187	5.4	118	25	-	203
KO2	MS	61.93	0.91	16.12	7.22	0.18	2.89	1.40	5.34	1.29	0.20	2.19	99.66	-	383	36	7	18	6	5	8	27	24.8	119	3.4	144	34	-	128
KO3	TUFF	61.86	0.83	15.97	7.40	0.20	3.17	1.62	5.16	1.17	0.16	2.29	99.83	-	398	38	8	19	6	5	6	23	24.4	130	3.2	140	31	-	130
KO4	VFS	66.87	0.67	15.38	4.46	0.12	2.25	1.13	4.18	2.43	0.11	2.03	99.64	-	676	85	22	18	13	10	1	70	12.8	119	8.3	80	31	-	302
<i>Koura Formation, quarry road outcrop, Mihonoseki</i>																													
KO6	FS	67.21	0.63	14.38	5.31	0.09	2.06	1.87	3.09	2.17	0.15	2.75	99.70	-	816	76	20	15	9	10	17	63	12.1	256	7.7	86	30	-	255
KO5	AND	53.40	1.46	15.36	11.30	0.18	6.67	2.39	3.30	1.11	0.28	4.14	99.59	-	414	38	36	19	5	16	5	23	33.6	206	2.5	308	31	-	133

**NOTES:** Column headings: SANR=sample number; LITH=lithology; LOI=loss on ignition. Dash (-): not determined.

Codes: LITH: CS=coarse sand; MS=medium sand; FS=fine sand; VFS=very fine sand; ZST=siltstone; MST=mudstone; MST-C=mudstone clast; BAS=basalt; WBAS=weathered basalt; AND=andesite.

Normalised elemental abundances of the Omori Formation lavas and volcanic clasts analysed from the Izumo area show patterns most similar to the felsic igneous rock average of Condie (1993). Although abundances in the segment Nb–Ce are <UCC and are often lower than the felsic rock average, they are strongly depleted in Ni, Cr, and V (Fig. 4 A), and are thus clearly distinct from more mafic andesite and basalt. On a total-alkali-silica classification diagram, the Omori lavas are all classified as dacites. This is supported by the multi-element patterns.

Representative samples of sediments from the Omori, Fujina and Jinzai Formations in the area south of Lake Jinzai show contrasting patterns on multi-element diagrams (Fig. 5). Sandstones from an example locality in the Omori Formation have patterns that correspond very closely with Omori dacites (Fig. 5A). The single mudstone analysed also has an identical pattern, illustrating the lack of sorting fractionation in these proximal volcanoclastic sediments. The close match with the dacite patterns is repeated at the other localities sampled, and the Omori sediments in this area were clearly derived from the dacites on which they rest.

Sandstones and mudstones from the overlying Fujina Formation exhibit different patterns, with abundances of most elements in the sandstones lying below UCC (Fig. 5B). They are also distinguished by marked depletion in Ca, Na and Sr, and compatible element abundances similar to UCC, in sharp contrast to the Omori sediments. Patterns in mudstones vary, but differ slightly from the sandstones. Depletion in Ca, Na and Sr is slightly greater than in the sands, and normalised abundances in the segment Ce–V are generally >UCC, in contrast to depletion in the sands. This suggests some sorting fractionation has occurred between sand and mud. The change in pattern from the Omori Formation also suggests that the source of the Fujina sediments differed. Although the flatter patterns could imply a more mafic (andesitic) source, the patterns also resemble Phanerozoic TTG, and a plutonic component may also be present. This is supported by the greater SiO<sub>2</sub> contents in Fujina sandstones (up to 83 wt%; Table 1A) compared to those for the Omori Formation (all <70 wt%). Depletion in Ca, Na and Sr is likely to be a weathering effect, as all three elements are susceptible to mobilization in surficial weathering.

Samples collected from the Jinzai Formation in the area of the Jinzai Basalt also show clearly differing patterns from the above. Two samples of Jinzai Basalt breccia are enriched in Ca, Sr, Mg and Ce relative to UCC, and also show progressive enrichment in the elements Sc–V (Fig. 5C). Their pattern is thus comparable to that of average Mesozoic–Cenozoic basalt (Fig. 4A). With one exception, sandstones and mudstones collected from the vicinity of the Jinzai Basalt cone display the same patterns as the basalts, with marked enrichment in the segment Sc–V, as well as positive Ca, Sr, Mg and Ce anomalies. This reflects a

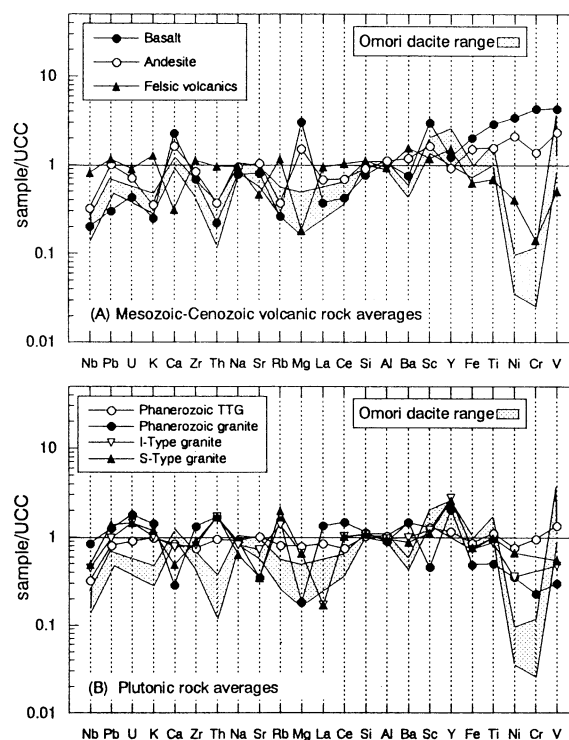


Fig. 4. UCC-normalized multi-element plots for published volcanic and plutonic rock averages compared to the range of Omori Formation dacites analysed in this study. A: Mesozoic–Cenozoic volcanic rock averages (Condie 1993); B: Phanerozoic TTG (tonalite–trondhjemite–granodiorite) and granite (Condie 1993), and average I- and S-type granite (Whalen et al., 1987). Omori dacite range covers all Omori dacite lavas and clasts listed in Table 1. Major elements (K, Ca, Na, Mg, Si, Al, Fe, Ti) are normalized as oxides.

substantial fragmental basaltic component, at least locally. The exceptional sample (S-25) has a pattern comparable to the Omori Formation dacites and sediments, suggesting that influxes of primarily dacitic sediment still occurred at this time.

Jinzai Formation sandstones and mudstones from localities stratigraphically above the Jinzai Basalt horizon show patterns similar to those of the Fujina Formation, with abundances of nearly all elements <UCC, and significant depletion in Ca, Na and Sr (Fig. 5 D). Compatible elements are again similar to UCC. Mudstones are rather more fractionated than in the Fujina Formation, with marked enrichment in Sc–V, and clear separation from their companion sands. This suggests that sorting is rather more advanced in the Upper Jinzai sediments than in the Fujina Formation. SiO<sub>2</sub> contents in the Upper Jinzai sandstones are generally greater than in the Fujina Formation (77–84 wt%; Table 1A), and the patterns again suggest a significant plutonic component. This is also supported by estimates of detrital lithic populations (Tateishi, *in prep.*), which reveal significant quantities of unitary quartz, plagioclase and K-feldspar and fewer rock fragments than in Omori equivalents.

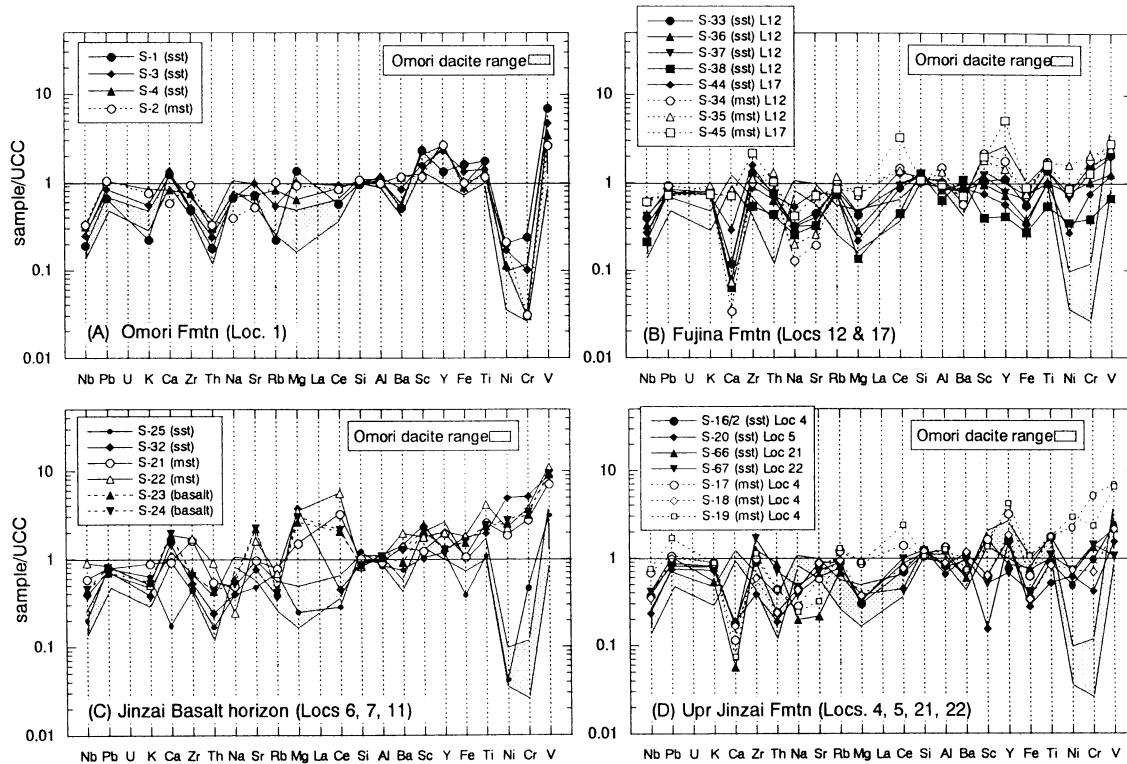


Fig. 5. UCC-normalized multi-element plots for representative samples from the Omori, Fujina and Jinzai Formations in the area south of Lake Jinzai, Izumo district, compared to Omori dacite. Data from Table 1 A; localities shown on Figure 3.

Samples from the Nishi-Izumo area to the east show some stratigraphic variation. This area was mapped as Fujina Formation by Kano *et al.* (1997). Those from the base of the section (Loc. 18; Fig. 6A) display patterns most similar to Omori Formation sediments and dacites (Fig. 5A). Those from Loc. 19 (stratigraphically higher) display patterns similar (Fig. 6B) to the Fujina and Upper Jinzai suites (Figs. 5B & D), suggesting that plutonic detritus may then have been supplied. Abundances in sandstones are generally  $<UCC$ , except for Zr, Si and V, and marked depletion is evident for Ca. Mudstones show higher abundances in the segment Sc-V, as do the Fujina and Upper Jinzai suites. These contrasts between the two Izumo localities suggests that distinct changes in provenance may occur at equivalent horizons over quite short distances, presumably as a result of lateral facies variation and the influence of local catchment geology.

Medium-grained sandstones from the Matsue Formation (Shimada drillcore) display patterns (Fig. 7A) which clearly differ from their correlatives in the Jinzai Formation. Only  $SiO_2$  is enriched relative to UCC, and many elements (Ca, Th, Mg, Ce, Sc-V) are quite strongly depleted ( $0.2-0.5 \times UCC$ ). Fine- and very fine-grained sandstones display similar patterns (not shown), but tend to be slightly less depleted. In contrast, mudstones display linear patterns close to UCC composition, except for clear depletion in Ca, Na and Sr, and slight and progressive enrichment in the compatible element segment Fe-V. The contrasts in the

patterns of the medium sandstones and mudstones are attributable to sorting and winnowing in the very shallow marine embayment in which the Matsue Formation is considered to have been deposited (Nakayama *et al.*, 1996). Elevated  $SiO_2$  contents in the sandstones (many  $>80 \text{ wt}\%$ ; Table 2), marked Ca, Na and Sr depletion, and the flat patterns suggest derivation from moderately weathered, largely plutonic (granodioritic) source.

Outcrop samples of Matsue Formation in the Nanpeidai area of Matsue City display similar patterns to those above, but with larger Ca, Na and Sr anomalies (Fig. 8). Alkalic Matsue Formation basalt sampled from road outcrop (Fig. 8a) has a pattern similar to Jinzai Basalt (Fig. 5C), with Zr, Mg and Ce greater than UCC, and progressive enrichment in the segment Sc-V. This pattern is replicated in overlying weathered basalt, except that Nb, Pb and Al are enriched, and K, Ca, Na, Sr and Rb are strongly depleted relative to UCC. Although Ca, Na and Sr are also strongly depleted in the overlying sandstones, no other signals of a basaltic component (e.g. Mg or Sc-V enrichment) are apparent in their patterns (Fig. 8A). This suggests that little basaltic detritus was recycled into the overlying sedimentary pile in this case.

Sandstones and mudstones from quarry outcrop at Nanpeidai (locality of Nakayama *et al.*, 1996) show comparable multi-element patterns to the other Matsue Formation localities, with abundances of all elements except  $SiO_2$  less than in UCC (Fig. 8B). Depletion in Ca, Na and Sr

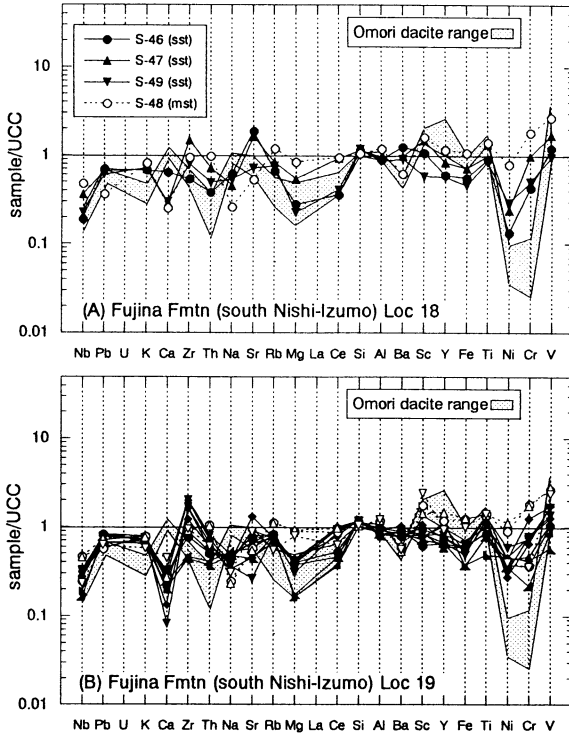


**Fig. 6.** UCC-normalised multi-element plots for sandstones and mudstones from the Fujina Formation in south Nishi-Izumo district, compared to Omori dacite. Data from Table 1B. Location 18 (A) is stratigraphically below location 19 (B).

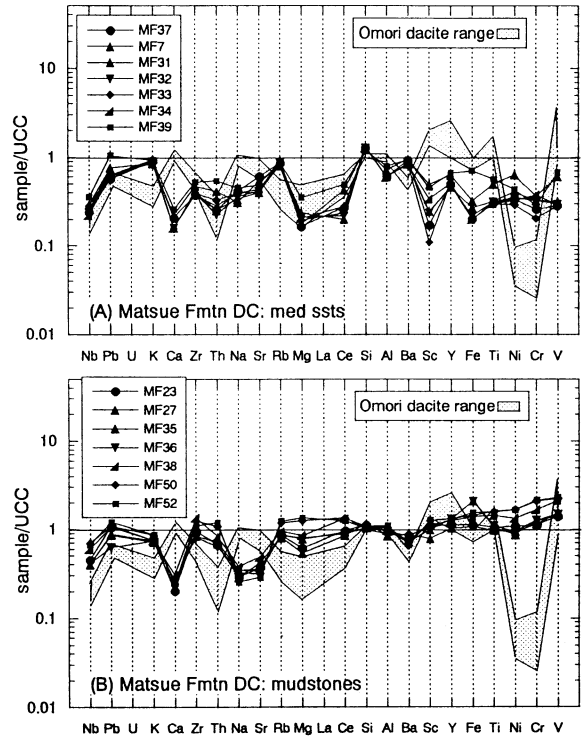


**Fig. 7.** UCC-normalized multi-element plots for (A) medium-grained sandstones and (B) mudstones from the Matsue Formation, Shimada drillcore, Matsue City. Data from Table 2.

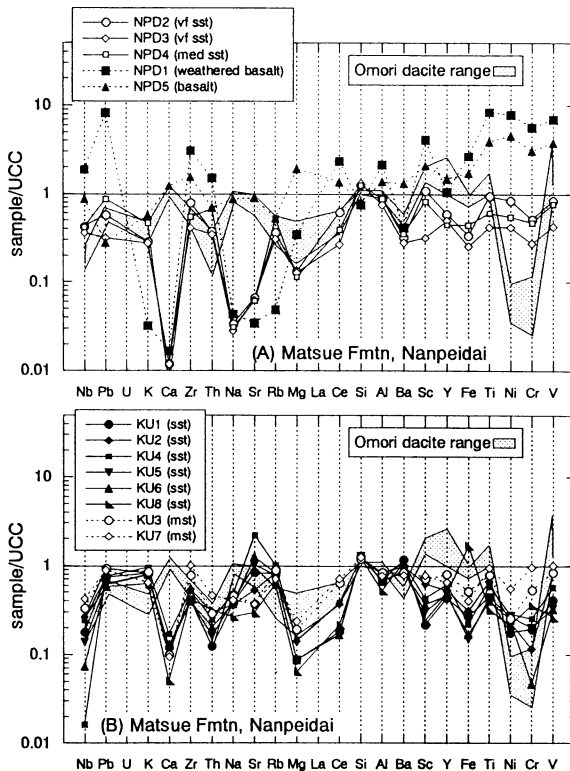


**Fig. 8.** UCC-normalized multi-element plots for (A) Matsue Formation alkalic basalts and sandstones, road outcrop, Nanpeidai, Matsue City; (B) Matsue Formation sandstones and mudstones from quarry outcrop, Nanpeidai, Matsue City (locality of Nakayama et al., 1996). Data from Table 3 A.

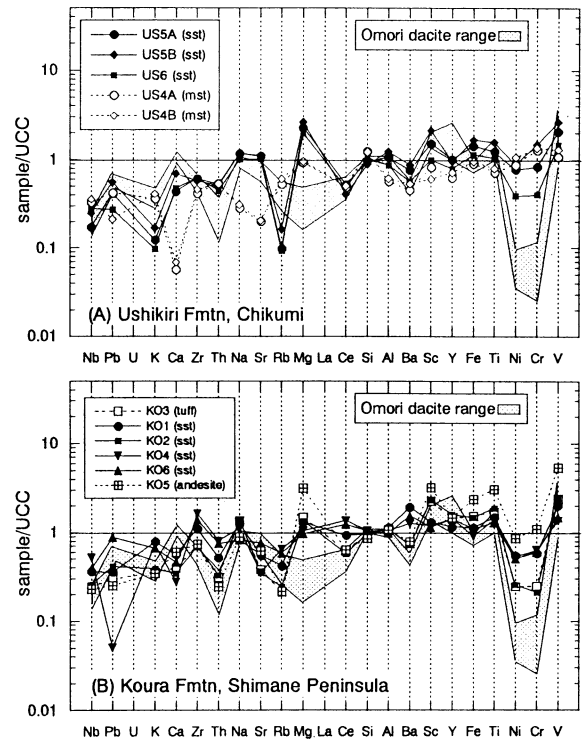


**Fig. 9.** UCC-normalized multi-element plots for (A) Turbidite sandstones and mudstones, Ushikiri Formation, Chikumi, eastern Shimane Peninsula; (B) non-marine sandstones and a tuff from the Koura Formation, Karuba, and a Koura andesite. Data from Table 3 B.

is, however, intermediate between that in the Shimada drillcore samples and the other Nanpeidai samples. This suggests that differing parts of the Matsue Formation were fed from sources where intensity of weathering varied. Alternatively, intensity of secondary surficial weathering during and immediately after deposition may have varied within the depositional basin.

Turbidite sandstones and mudstones from the eastern block of Ushikiri Formation at Chikumi (Table 3B) display differing patterns from all the above suites (Fig. 9A). With the exception of depletion in Ca, Sr and Rb in a few samples, slopes tend to increase from left to right, with abundances near to or slightly greater than UCC in the segment Sc-V. The pattern closely resembles that of average Mesozoic-Cenozoic andesite (Fig. 4A), and implies a predominantly andesitic source. This is in accord with the volcanoclastic nature of Ushikiri turbidites, and the moderate SiO<sub>2</sub> contents (55–68 wt%) of three of the four sandstones analysed from this locality. Ushikiri mudstones also show similar patterns to the sandstones, reflecting the lack of sorting fractionation characteristic of volcanoclastic sediments. The andesitic Ushikiri patterns contrast sharply with the dacitic patterns observed in their time correlatives in the Izumo Omori Formation suite, suggesting they did not have the same source. This confirms the paleocurrent evidence that the eastern block of the Ushikiri Formation had a different source from that in west Shimane Peninsula. The Chikumi Ushikiri outcrop therefore does not represent a deeper-water equivalent of the Omori Formation exposed along the southern edge of Lake Shinji. Much more extensive sampling is required to characterize the spatial variability in the Ushikiri and Omori Formations, however.

The small suite of sandstones analysed from the non-marine Koura Formation (Early Miocene) have patterns which lie between those of an interbedded tuff and an andesite (Fig. 9B). Depletion in the mobile elements (Ca, Na, Sr) is not evident, suggesting that the Koura sediments were derived from a relatively unweathered source terrane. The patterns themselves suggest that the source consisted primarily of andesite, along with lesser more felsic volcanic rocks and tuffs.

### Conclusions

Clear contrasts in multi-element abundance patterns occur between the Miocene sedimentary formations examined here. Sandstones from the Koura Formation, the oldest unit represented, display patterns indicative of derivation from coeval andesitic and felsic volcanic source rocks. Turbidite sandstones from the Ushikiri Formation in Shimane Peninsula also display andesitic signatures, in contrast to the strongly dacitic patterns of lateral equivalents in the shallower-water Omori Formation from the Izumo area. The succeeding Fujina Formation in that area exhibits more depleted patterns relative to UCC, suggestive of some

influx of weathered plutonic detritus. Some lateral or stratigraphic variation is indicated by additional Fujina samples from the South Nishi-Izumo area. Depleted patterns and probable plutonic input is also recognised in the Jinzai Formation, except in the immediate vicinity of the Jinzai Basalt edifice, where geochemical signatures of basaltic detritus appear in the sediments. Equivalents in the Matsue Formation also show depleted abundances relative to UCC, but patterns differ from those of the Jinzai Formation, especially with respect to elements mobile during weathering. A mainly plutonic source is inferred, with additional modification due to source weathering and sedimentary processes associated with deposition in a protected shallow marine embayment.

Although interpretation of this data has just begun, the preliminary results presented here suggest sediments deposited in backarc settings can show marked stratigraphic and lateral geochemical variation. This is a consequence of their proximal deposition, the complexity of the hinterland geology, and the influence of small catchments.

### Acknowledgements

This work was begun with Katsuhiro Nakayama as the first step in a joint investigation of the geochemistry of the Miocene sediments in the area. His sedimentological expertise and enthusiasm will be greatly missed. Our thanks also to Akio Iwata of Shimada Technical Consultants Ltd. for giving access to the Matsue Formation drillcore, to Seiki Yamauchi and Yosuke Bandou for discussions on various aspects of the geology of the areas sampled, and to Yoshihiro Sawada for access to the XRF. This work was partly supported by a Monbukagakusho grant-in-aid (13440147) to B.P. Roser.

### References

- Condie, K.C. 1993. Chemical composition and evolution of the upper continental crust: Contrasting results from surface samples and shales. *Chemical Geology*, **104**, 1-37.
- Dinelli, E., Lucchini, F., Mordenti, A. and Paganelli, L. 1999. Geochemistry of Oligocene-Miocene sandstones of the northern Apennines (Italy) and evolution of chemical features in relation to provenance changes. *Sedimentary Geology*, **127**, 193-207.
- Editorial Board of Geological map of Shimane Prefecture (EBGMSP) 1997. Geological map of Shimane Prefecture (1:200,000).
- Kano, K. 1998. A shallow-marine alkali-basalt tuff cone in the Middle Miocene Jinzai Formation, Izumo, SW Japan. *Journal of Volcanology and Geothermal Research*, **87**, 173-191.
- Kano, K. and Nakano, S. 1986. *Geology of the Etomo district*. With geological sheet map at a scale of 1:50,000. Tsukuba, Geological Survey of Japan, 30 p.\*
- Kano, K., Takeuchi, K., Oshima, K. and Bunno, M. 1989. *Geology of the Taisha district*. With geological sheet map at a scale of 1:50,000. Tsukuba, Geological Survey of Japan, 58 p.\*
- Kano, K., Takeuchi, K. and Matsuura, H. 1991. *Geology of the Imaichi district*. With geological sheet map at a scale of 1:50,000. Tsukuba, Geological Survey of Japan, 79 p.\*
- Kano, K., Yamauchi, S., Takayasu, K., Matsuura, H. and Bunno, M. 1994.

- Geology of the Matsue district*. With geological sheet map at a scale of 1:50,000. Tsukuba, Geological Survey of Japan, 126 p.\*
- Kano, K., Matsuura, H., Sawada, Y. and Takeuchi, K. 1997. *Geology of the Iwami-Oda and Oura districts*. With geological sheet map at a scale of 1:50,000. Tsukuba, Geological Survey of Japan, 118 p.\*
- Kimura, J.-I. and Yamada, Y. 1996. Evaluation of major and trace element analyses using a flux to sample ratio of two to one glass beads. *Journal of Mineralogy, Petrology and Economic Geology*, **91**, 62-72.
- Morita, H. and Nakayama, K. 1999. Stratigraphy of the Middle Miocene in the southwestern part of Izumo City in Shimane Prefecture of SW Japan, and subsiding properties of its sedimentary basin. *Geoscience Reports of Shimane University*, **18**, 25-39.
- Morris, P.A. and Itaya, T. 1997. The Matsue Formation: Evidence for gross mantle heterogeneity beneath Southwest Japan at 11 Ma. *The Island Arc*, **6**, 337-352.
- Nakayama, K. 1997. Unidirectional to bidirectional suttidal sandwaves influenced by gradually decreasing steady flow velocity. *Geological Magazine*, **134**, 557-561.
- Nakayama, K., Kan, S., Takayasu, K. and Sampei, Y. 1996. Tidal sand waves in the Miocene Matsue Formation in Shimane Prefecture, Japan. *Journal of the Geological Society of Japan*, **102**, 379-390.\*
- Norrish, K. and Hutton, J.T., 1969. An accurate X-ray spectrographic method for the analysis of a wide range of geological samples. *Geochimica et Cosmochimica Acta*, **33**, 431-453.
- Roser, B.P., Kimura, J.-I. and Hisatomi, K. 2000. Whole-rock elemental abundances in sandstones and mudrocks from the Tanabe Group, Kii Peninsula, Japan. *Geoscience Reports of Shimane University*, **19**, 101-112.
- Roser, B.P., Sawada, Y. and Kabeto, K. 1998. Crushing performance and contamination trials of a tungsten carbide ring mill compared to agate grinding. *Geoscience Reports of Shimane University*, **17**, 1-11.
- Takayasu, K. 1986. Diversification in the molluscan fauna of the Miocene Izumo Group, San-in district, southwest Japan. *Paleontological Society of Japan Special Paper*, **29**, 173-186.
- Takayasu, K. and Sawada, Y. 1989. A new aspect on the age of alkaline basalt from Izumo Group, Shimane Prefecture, Southwest Japan. In: I. Kobayashi and M. Tateishi (eds) "Paleo-Japan sea: Paleoenvironmental change and stratigraphy of the upper Cenozoic along the Japan sea coast", Niigata University, pp 78-79.\*\*
- Taylor, S.R. and McLennan, S.M. 1985. The continental crust: its composition and evolution. Oxford, Blackwell Scientific, 312 pp.
- Whalen, J.B., Currie, F.L. and Chappell, B.W. 1987. A-type granities: geochemical characteristics, discrimination and petrogenesis. *Contributions to Mineralogy and Petrology*, **95**, 407-419.
- Yamauchi, S., Mitsunashi, T. and Yamamoto, Y. 1980. Miocene systems in Shimane Peninsula. Excursion guidebook, second course. *Geological Society of Japan, 87th Annual Meeting, Matsue, 1980*. 39 pp.\*\*
- Yamauchi, S. and Yoshitani, A. 1981. Tectonic movements in the progressive stage of the Green-Tuff basins-Taking the case of the Miocene series in the eastern part of Shimane Prefecture, western Japan. *Journal of the Geological Society of Japan*, **87**, 711-724.\*

\* In Japanese, English abstract or summary.

\*\* In Japanese.

(Received: 10 Dec. 2001, Accepted: 17 Dec. 2001)

(要 旨)

Barry Roser・立石陽子・中山勝博, 出雲-松江地域および島根半島の中新世堆積岩/火山岩の全岩元素組成, 島根大学地球資源環境学研究報告, 20, 69-82

出雲-松江地域および島根半島では, 中新世の背弧海盆に堆積した碎屑岩類が, 海岸線沿いの連続露頭に広く見出しされる。この地域に分布する古浦層, 牛切層, 大森層, 布志名層および松江層から採取した砂岩, 泥質岩とそれに伴う火山岩類 147 試料について, 今回新たに XRF 分析を行った。その結果, 堆積学的に見て比較的短期間に, かなりの組成変化があることがわかった。Upper Continental Crust (UCC) で規格化された結果から見ると, 古浦層砂岩は, 互層する酸性凝灰岩および同時代の安山岩の中間の値を示す。千酌海岸の牛切層タービダイトも安山岩のパターンを持つが, 出雲付近に分布する大森層中の浅海層はデイサイト質火山岩起源を示す。その上位層である布志名層は全般に UCC よりも低い元素組成を持ち, このことは風化した深成岩碎屑物の影響を示唆している。同様な傾向は松江層に対比される神西層にも見られるが, 例外的に神西層内では地域的な玄武岩の影響も見られる。松江層は深成岩起源を示す低いパターンを持つが, 風化の影響が大きく, かつ浅海下に堆積した際の淘汰の影響を強く受けている。観察された層位的変化と側方変化は, 比較的近い堆積場, 供給源の複雑な地質, そして限られた集水域からの堆積物供給を反映したものと考えられる。